

Cosmological Constraints from Galaxy Cluster Statistics in KiDS

An overview on the cosmological results from KiDS-DR3 based on cluster statistics, and perspectives for the KiDS-DR4 analysis

Giorgio F. Lesci
giorgio.lesci2@unibo.it

AMICO clusters group in KiDS

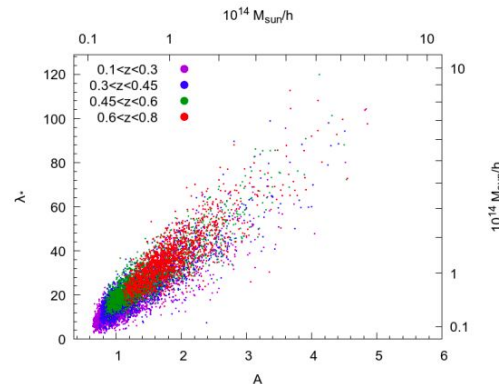
Group members:

S. Bardelli, G. Castignani, G. Covone, C. Giocoli, L. Ingoglia, G. F. Lesci, F. Marulli, M. Maturi, L. Moscardini, E. Puddu, M. Radovich, M. Romanello, M. Sereno, D. Tramonte

AMICO^{1,2} (Adaptive Matched Identifier of Clustered Objects) is our cluster detection algorithm. It is one of the two algorithms for cluster identification officially adopted by the Euclid mission.³

AMICO provides unbiased estimates of redshift and mass proxies.

Two mass proxies: **richness**, λ , and **signal amplitude**, A .



In addition, purity and completeness are estimated through mock catalogues², by applying the SinFoniA (Selection Function extrActor) algorithm.

¹ Bellagamba et al. 2018, <https://arxiv.org/abs/1705.03029>

² Maturi et al. 2019, <https://arxiv.org/abs/1810.02811>

³ Euclid Collaboration 2019,

AMICO clusters group in KiDS

Group members:

S. Bardelli, G. Castignani, G. Covone, C. Giocoli, L. Ingoglia, G. F. Lesci, F. Marulli, M. Maturi, L. Moscardini, E. Puddu, M. Radovich, M. Romanello, M. Sereno, D. Tramonte

Catalogue from KiDS-DR3: Maturi et al. 2019 (<https://arxiv.org/abs/1810.02811>)

Mass calibration in KiDS-DR3: Bellagamba et al. 2019 (<https://arxiv.org/abs/1810.02827>)

Many recent works based on KiDS-DR3 data...

Cosmology:

- Cosmological constraints from 2-halo term of WL stacked profiles (Giocoli et al. 2021, <https://arxiv.org/abs/2103.05653>; Ingoglia et al. 2022, <https://arxiv.org/abs/2201.01545>)
- Cluster counts (Lesci et al. 2022a, <https://arxiv.org/abs/2012.12273>)
- Cluster 3D clustering (Lesci et al. 2022b, <https://arxiv.org/abs/2203.07398>)
- Cluster 2D clustering (Romanello et al. in prep.)

Astrophysics:

- Intrinsic scatter in stacked relations (Sereno et al. 2020, <https://arxiv.org/abs/2006.16264>)
- Galaxy population properties and their redshift dependence (Radovich et al. 2020, <https://arxiv.org/abs/2009.03563>)
- Evolution of the luminosity function between $z=0.1$ and $z=0.8$ (Puddu et al. 2020, <https://arxiv.org/abs/2011.05131>)
- Star forming and gas rich brightest cluster galaxies at $z \sim 0.4$ (Castignani et al. 2022, <https://arxiv.org/abs/2207.12073>)
- Mass and redshift dependence of cluster pressure profile with stacks on SZ maps (Tramonte et al. 2023, <https://arxiv.org/abs/2302.06266>)

... and additional papers in preparation based on KiDS-DR4!

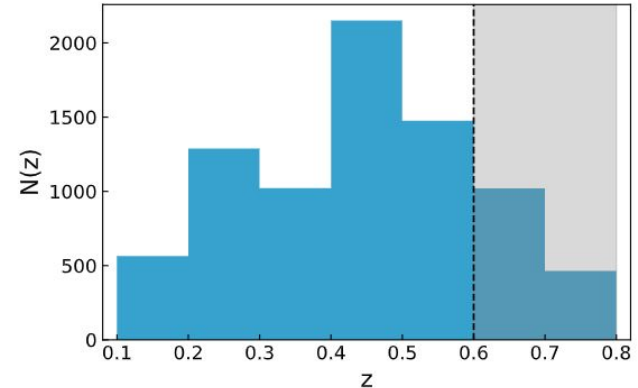
AMICO clusters in KiDS-DR3

Third data release of the Kilo Degree Survey (KiDS-DR3),
carried out with the VLT Survey Telescope.

DR3: Photometry in u , g , r , i bands.

AMICO KiDS-DR3 sample of galaxy clusters (**Maturi et al. 2019**):

- Effective area: 377 deg²;
- $z \in [0.1, 0.8]$;
- 7988 clusters (3652 in the counts analysis).



Redshift distribution of the AMICO clusters in KiDS-DR3. Objects with $z > 0.6$, not considered in the cluster counts analysis, are covered by the grey shaded area.

AMICO clusters in KiDS-DR3

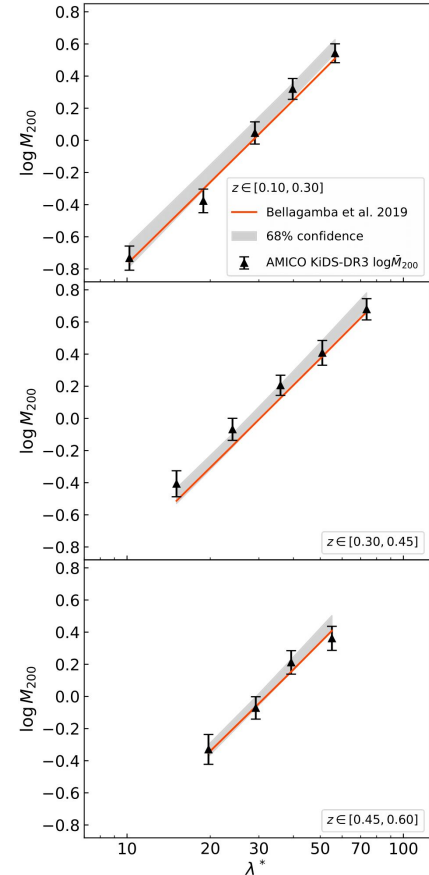
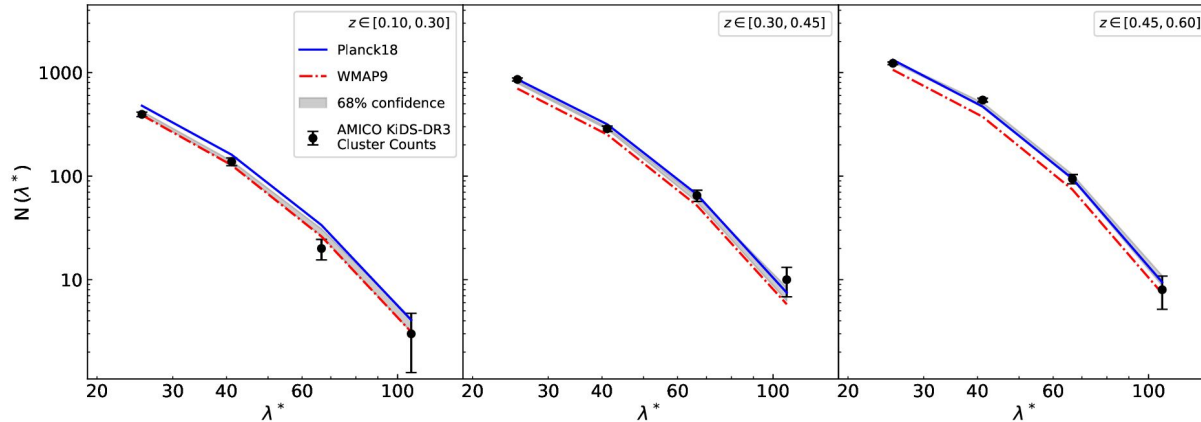
Cluster counts (Lesci et al. 2022a)

Joint analysis of cluster counts and stacked weak lensing: flat priors on Ω_m , σ_8 , and on the parameters of the mass-richness relation.

Scaling relation:

$$\log \frac{M_{200}}{10^{14} M_\odot / h} = \alpha + \beta \log \frac{\lambda^*}{\lambda_{piv}^*} + \gamma \log \frac{E(z)}{E(z_{piv})} \rightarrow \text{we derived stacked masses first}$$

Strong constraints on the mass-richness relation and S_8 .



AMICO clusters in KiDS-DR3

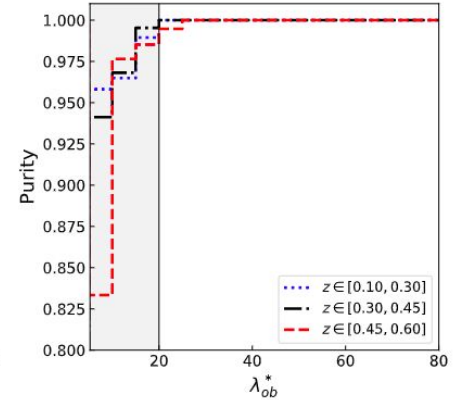
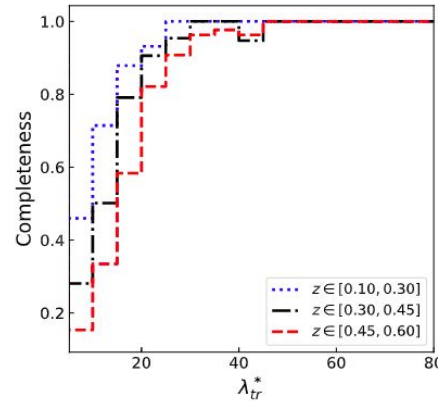
Cluster counts (Lesci et al. 2022a)

Counts model:

$$\begin{aligned}
 \langle N(\Delta\lambda_{ob,i}^*, \Delta z_{ob,j}) \rangle &= w(\Delta\lambda_{ob,i}^*, \Delta z_{ob,j}) \Omega \int_0^\infty dz_{tr} \frac{dV}{dz_{tr} d\Omega} \times \\
 &\times \int_0^\infty dM_{tr} \frac{dn(M_{tr}, z_{tr})}{dM_{tr}} \int_0^\infty d\lambda_{tr}^* P(\lambda_{tr}^* | M_{tr}, z_{tr}) \times \\
 &\times \int_{\Delta z_{ob,j}} dz_{ob} P(z_{ob} | z_{tr, corr}) \int_{\Delta\lambda_{ob,i}^*} d\lambda_{ob}^* P(\lambda_{ob}^* | \lambda_{tr}^*),
 \end{aligned}$$

selection function

We estimated AMICO selection purity and completeness



Completeness: number of detections correctly identified as clusters over the total number of mock clusters.

-> that's why it is a function of true richness.

Purity: fraction of detections matching the clusters in the mock catalogue, over the total number of detections.

AMICO clusters in KiDS-DR3

Cluster counts (Lesci et al. 2022a)

Counts model:

$$\langle N(\Delta\lambda_{\text{ob},i}^*, \Delta z_{\text{ob},j}) \rangle = \underbrace{w(\Delta\lambda_{\text{ob},i}^*, \Delta z_{\text{ob},j})}_{\text{selection function}} \Omega \int_0^\infty dz_{\text{tr}} \frac{dV}{dz_{\text{tr}} d\Omega} \times$$
$$\times \int_0^\infty dM_{\text{tr}} \frac{dn(M_{\text{tr}}, z_{\text{tr}})}{dM_{\text{tr}}} \int_0^\infty d\lambda_{\text{tr}}^* P(\lambda_{\text{tr}}^* | M_{\text{tr}}, z_{\text{tr}}) \times$$
$$\times \int_{\Delta z_{\text{ob},j}} dz_{\text{ob}} P(z_{\text{ob}} | z_{\text{tr}, \text{corr}}) \int_{\Delta\lambda_{\text{ob},i}^*} d\lambda_{\text{ob}}^* P(\lambda_{\text{ob}}^* | \lambda_{\text{tr}}^*),$$

Build up a new cluster dataset:

- put the observed clusters in λ_{ob} bins;
- uniform extraction between 0 and 1 **for each observed cluster**: if the extracted number is lower than the λ_{ob} bin's purity, add the corresponding cluster to the new dataset;
- by accounting for $P(\lambda_{\text{tr}} | \lambda_{\text{ob}})$, weigh each cluster (in the new dataset) by the corresponding λ_{tr} bin completeness value;
- measure the (weighted) counts in this new dataset;
- the final weight, w , is just $(N \text{ in the original sample}) / (N \text{ in the new sample})$

AMICO clusters in KiDS-DR3

Cluster counts (Lesci et al. 2022a)

Counts likelihood:

matter density contrast
fluctuation

$$\mathcal{L}_{\text{counts}} = \int d\delta_{\text{b}}^{\# \text{ of } z \text{ bins}} \left[\prod_{i,j} \text{Pois} \left(N_{i,j} | \bar{N}_{i,j} + \frac{\partial N_{i,j}}{\partial \delta_{\text{b},j}} \delta_{\text{b},j} \right) \right] \mathcal{N}(\delta_{\text{b}} | 0, S) \longrightarrow$$

Convolution of Poissonian and Gaussian likelihoods, the latter encapsulating SSC effect (see Lacasa & Grain 2019)

$$\begin{aligned} \frac{\partial N_{i,j}}{\partial \delta_{\text{b},j}} &= w(\Delta\lambda_{\text{ob},i}^*, \Delta z_{\text{ob},j}) \Omega \int_0^\infty dz_{\text{tr}} \frac{dV}{dz_{\text{tr}} d\Omega} \times \\ &\times \int_0^\infty dM_{\text{tr}} \frac{dn(M_{\text{tr}}, z_{\text{tr}})}{dM_{\text{tr}}} b(M_{\text{tr}}, z_{\text{tr}}) \int_0^\infty d\lambda_{\text{tr}}^* P(\lambda_{\text{tr}}^* | M_{\text{tr}}, z_{\text{tr}}) \times \\ &\times \int_{\Delta z_{\text{ob},j}} dz_{\text{ob}} P(z_{\text{ob}} | z_{\text{tr}, \text{corr}}) \int_{\Delta \lambda_{\text{ob},i}^*} d\lambda_{\text{ob}}^* P(\lambda_{\text{ob}}^* | \lambda_{\text{tr}}^*), \end{aligned} \quad (14)$$

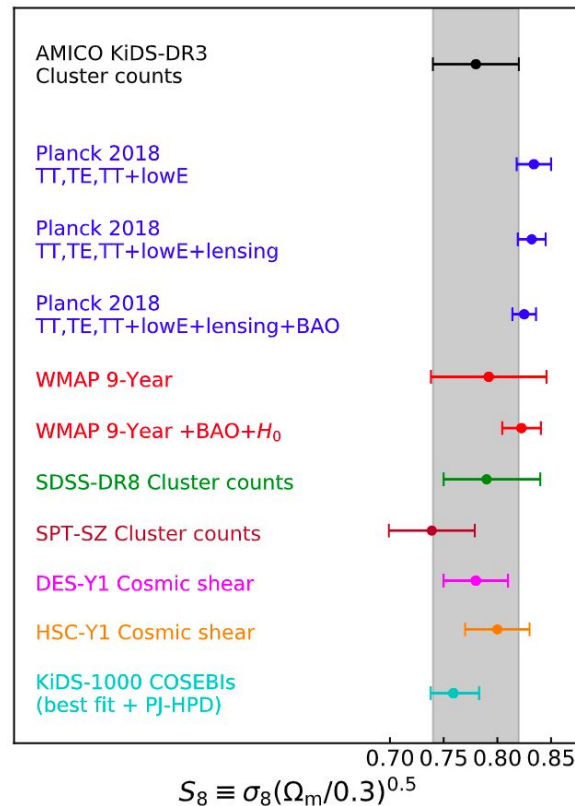
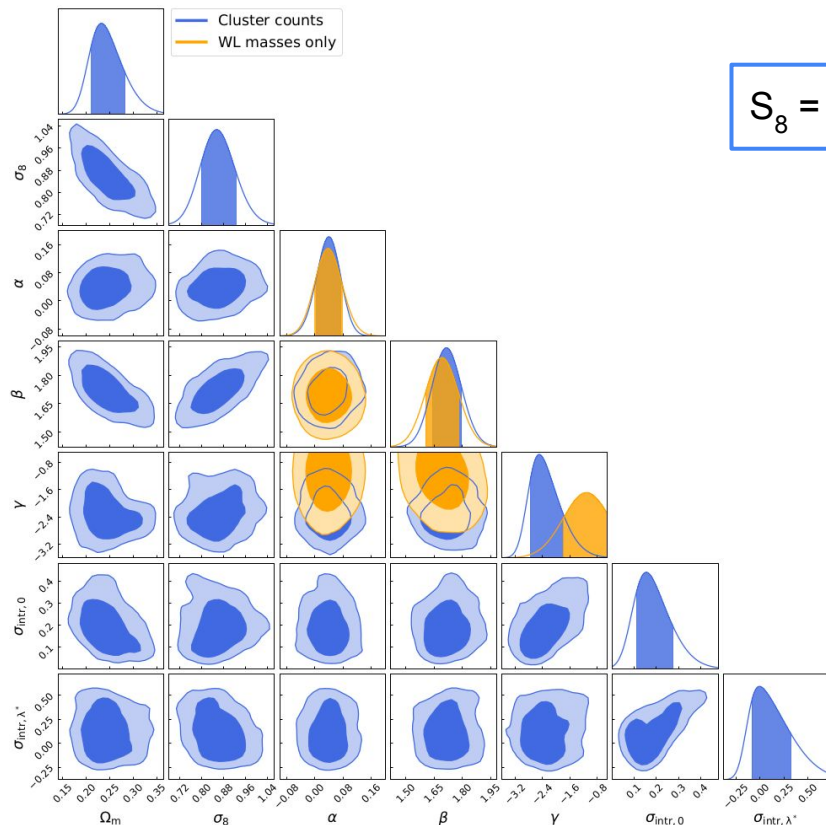
Probe response function

$$\ln \mathcal{L}'_{\text{counts}} = \ln \left[\prod_{i,j} \text{Pois} \left(N_{i,j} | \bar{N}_{i,j} + \frac{\partial N_{i,j}}{\partial \delta_{\text{b},j}} \delta_{\text{b},j} \right) \cdot \mathcal{N}(\delta_{\text{b}} | 0, S) \right] \longrightarrow$$

Computation-friendly likelihood form:
cosmology-dependent priors on δ_{b} , given by the S matrix (i.e. the covariance of the background matter density contrast)

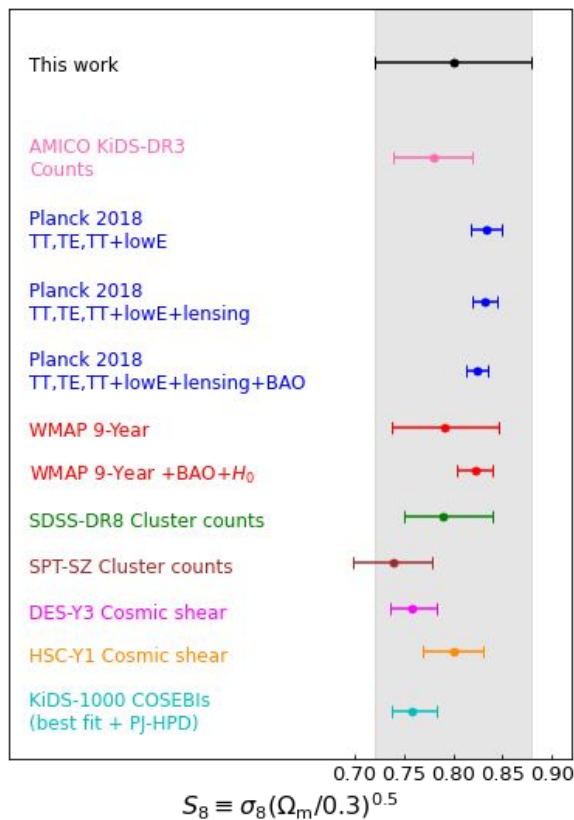
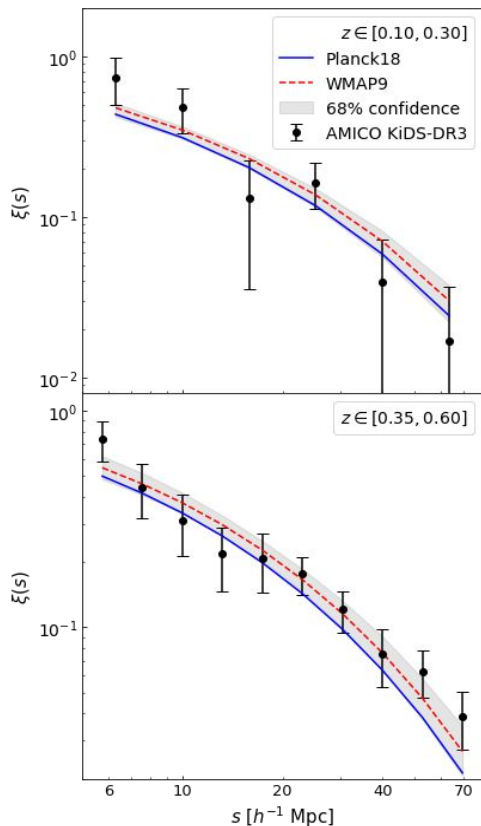
AMICO clusters in KiDS-DR3

Cluster counts (Lesci et al. 2022a)



AMICO clusters in KiDS-DR3

Cluster clustering (3D) (Lesci et al. 2022b)



$$S_8 = 0.80 \pm 0.08$$

Modelling of the 3D 2PCF monopole.

Effective bias:

$$b_{\text{eff}}(\Delta z_i) = \frac{1}{N_i} \sum_{j=1}^{N_i} \int_0^{\infty} dz \int_0^{\infty} d\lambda^* \int_0^{\infty} dM b(M, z) P(M|\lambda^*, z) \times P(z|z_{\text{obs},j}) P(\lambda^*|\lambda_{\text{obs},j}^*), \quad (10)$$

In particular, S_8 is marginalised over the scaling relation posteriors obtained from the counts+WL analysis.

In DR4: combination with counts. Simple combination in DR3: ~20% improvement on S_8 uncertainty.

AMICO clusters in KiDS-DR3

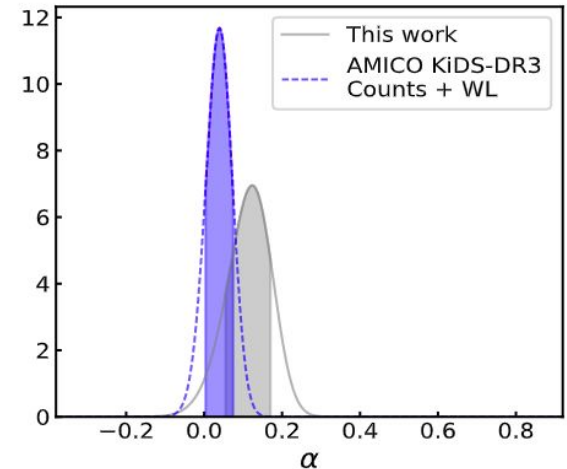
Cluster clustering (3D) (Lesci et al. 2022b)

With fixed cosmological parameters, it is possible to constrain the **normalisation of the mass-richness relation** (see also Chiu et al. 2020).

$$\log \frac{M_{200}}{10^{14} M_{\odot} / h} = \alpha + \beta \log \frac{\lambda^*}{\lambda_{piv}^*} + \gamma \log \frac{E(z)}{E(z_{piv})}$$

In this case we adopted Gaussian priors on β , γ , σ_{intr} , corresponding to the posteriors derived from the counts + WL analysis.

-> in combination with counts, cluster clustering may compensate the lack of weak lensing signal at high redshifts.

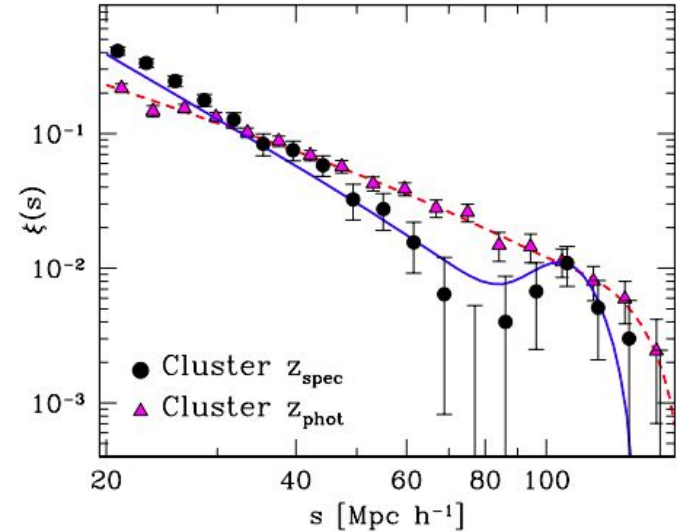


AMICO clusters in KiDS-DR3

Cluster 2D clustering and ξ_1 (Romanello et al. in prep.)

3D clustering: best choice in case of spectro-zs, for BAO modelling, but still a good choice for photometric catalogues of clusters (since the z uncertainty is lower compared to the galaxy photo- z errors).

2D clustering: we expect an excellent agreement with the 3D case, but which one is better in KiDS?



Veropalumbo et al. 2014

AMICO clusters in KiDS-DR3

Cluster 2D clustering and C_1 (Romanello et al. in prep.)

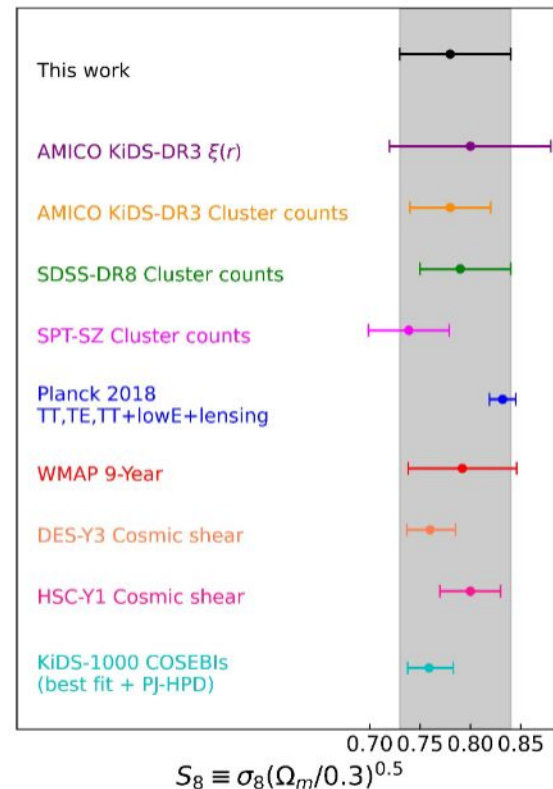
2D 2PCF ($w(\theta)$) better than 3D in KiDS-DR3.

C_1 s do not constrain σ_8 .

From simulations:

$w(\theta)$ better than C_1 s.

To be tested: $w(\theta)$ vs $\xi(r)$



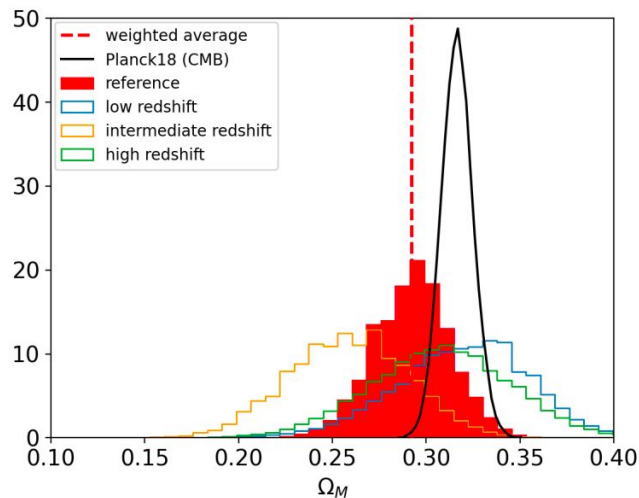
AMICO clusters in KiDS-DR3

Cosmology from cluster weak lensing 2-halo

Giocoli et al. 2021:

Ω_m from stacked weak lensing 2-halo term.

Competitive results, in agreement with Planck18.

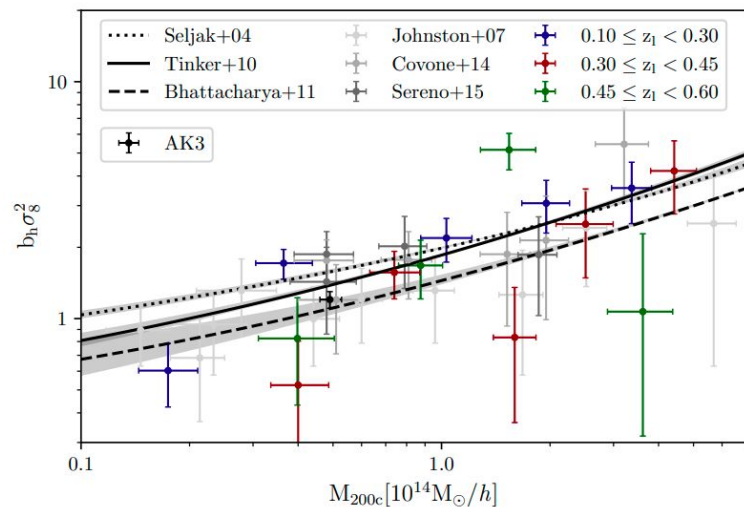


Ingoglia et al. 2022:

Halo bias-mass relation from stacked weak lensing 2-halo term.

Good agreement with theoretical and observational works.

Constraint on σ_8 by assuming Tinker+10 bias: $\sigma_8 = 0.63 \pm 0.10$
-> 2σ agreement with Planck18



AMICO clusters in KiDS-DR3

Splashback radius (Master Thesis by L. Palmucci)

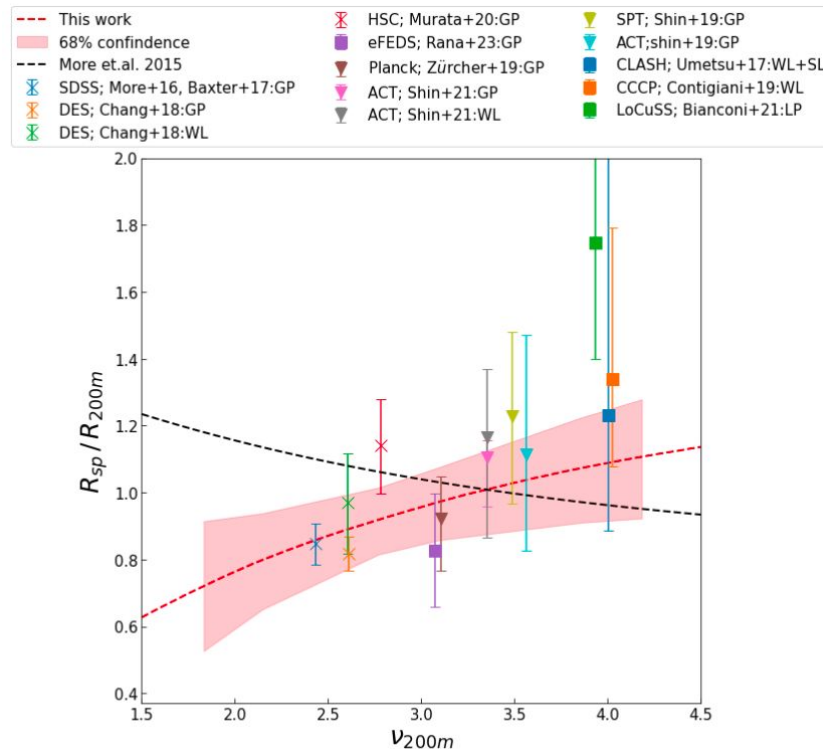
Based on the Diemer & Kravtsov 2014 model.

We simultaneously constrained masses and R_{sp} , by modelling $\Delta\Sigma_+$.

Specifically, given a set of halo profile parameters (i.e. at each MCMC step), R_{sp} was derived from the corresponding 3D density distribution.

Free parameters: mass, concentration, truncation radius, outer profile parameters.
Modelling up to $35 \text{ Mpc}/h$.

Right panel (inspired by Rana+23):
agreement with other observational works, discrepancies with More+15 at low ν .



AMICO clusters in KiDS-DR4

AMICO KiDS-DR4 catalogue: Maturi et al. in prep.

Observational improvements:

Five additional photometric bands ($ZYJHK_s$) from VIKING survey
-> huge improvement of the photo-zs.

Effective area: **840 deg²** (vs 377 deg² in KiDS-DR3).

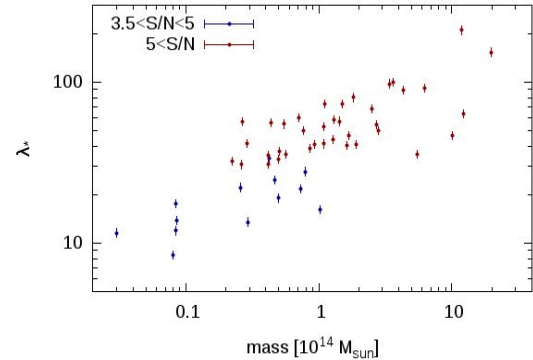
~ **25000 clusters** with S/N > 3.5 (vs ~8000 in DR3).

Reliable weak **lensing** signal **up to z = 0.8** (vs z < 0.6 in DR3).

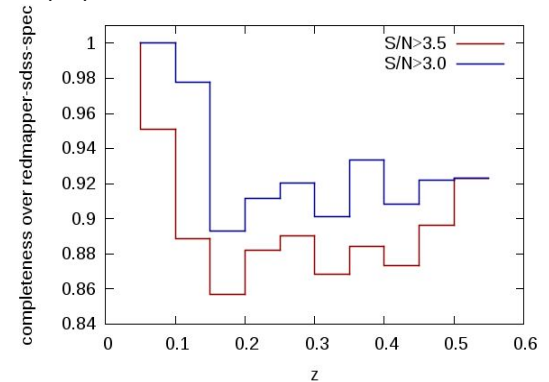
Improvements in the analysis:

Blinding.

Joint analysis of WL, counts and clustering.



X-ray observations (MCXC). Maturi et al. in prep.



Matching ratio over redMaPPer-SDSS-spec.
Maturi et al. in prep.

Unrequested digression: Blinding

Blinding: just another way to carry out the usual analyses (i.e. no scientific innovation is included) without being able to properly re-check what you did

Pros: surprise effect

Cons: I could not find any other pros

In the context of e.g. optical cluster analyses, we already know what to expect from the galaxy distribution.

Are we actually blind?

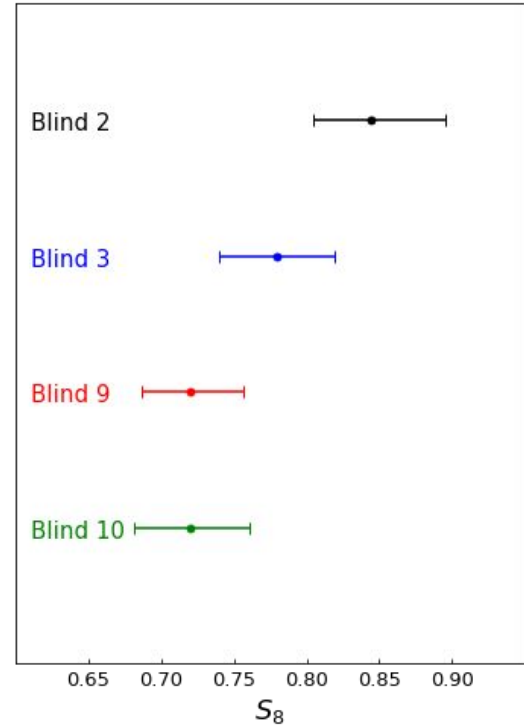
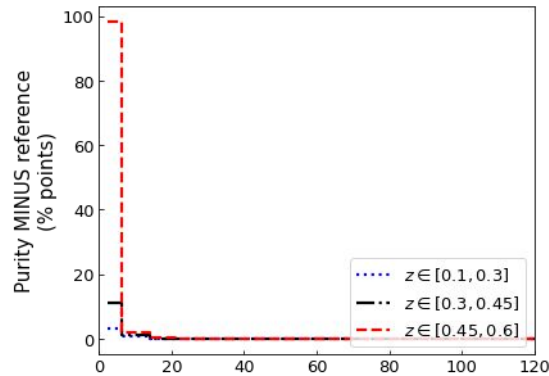
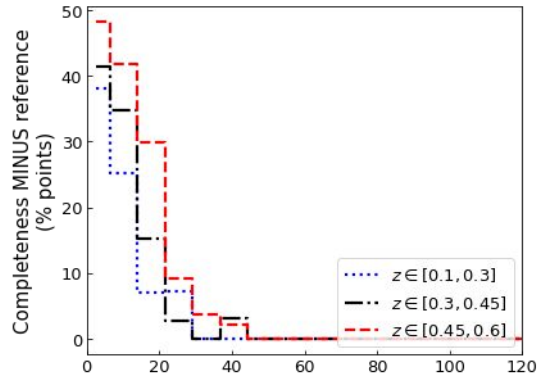
Perhaps the root of the problem is semantic: let's talk about 2sigma agreement instead of 2sigma tensions

Blinding in KiDS-DR4

Tests in KiDS-DR3

Blinding the AMICO completeness

Blind version 9



AMICO clusters in KiDS-DR4

Weak lensing mass calibration (Lesci et al. in prep. 1)

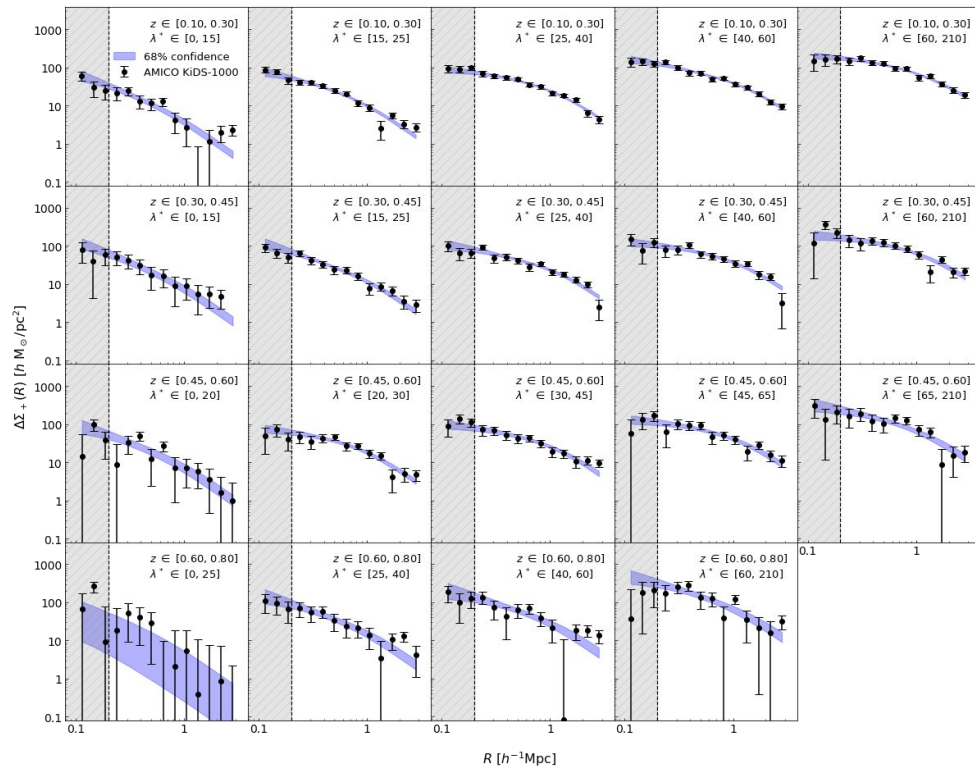
First step: deriving the M- λ scaling relation directly from the $\Delta\Sigma_+(R)$ stacked profiles.

$$\langle \Delta\Sigma(R_{\text{eff}}|\lambda_{\text{eff}}^*, z_{\text{eff}}) \rangle = \int_0^\infty dM \Delta\Sigma(R_{\text{eff}}|M, z_{\text{eff}}) P(M|\lambda_{\text{eff}}^*, z_{\text{eff}})$$

Advantages:

- the mass calibration depends on cosmology;
- the local properties of clusters are propagated into the cosmological posteriors...

... and with this regard, if we manage to constrain the M- λ relation through this modelling, for sure we can also constrain the mass-concentration (M-c) relation!



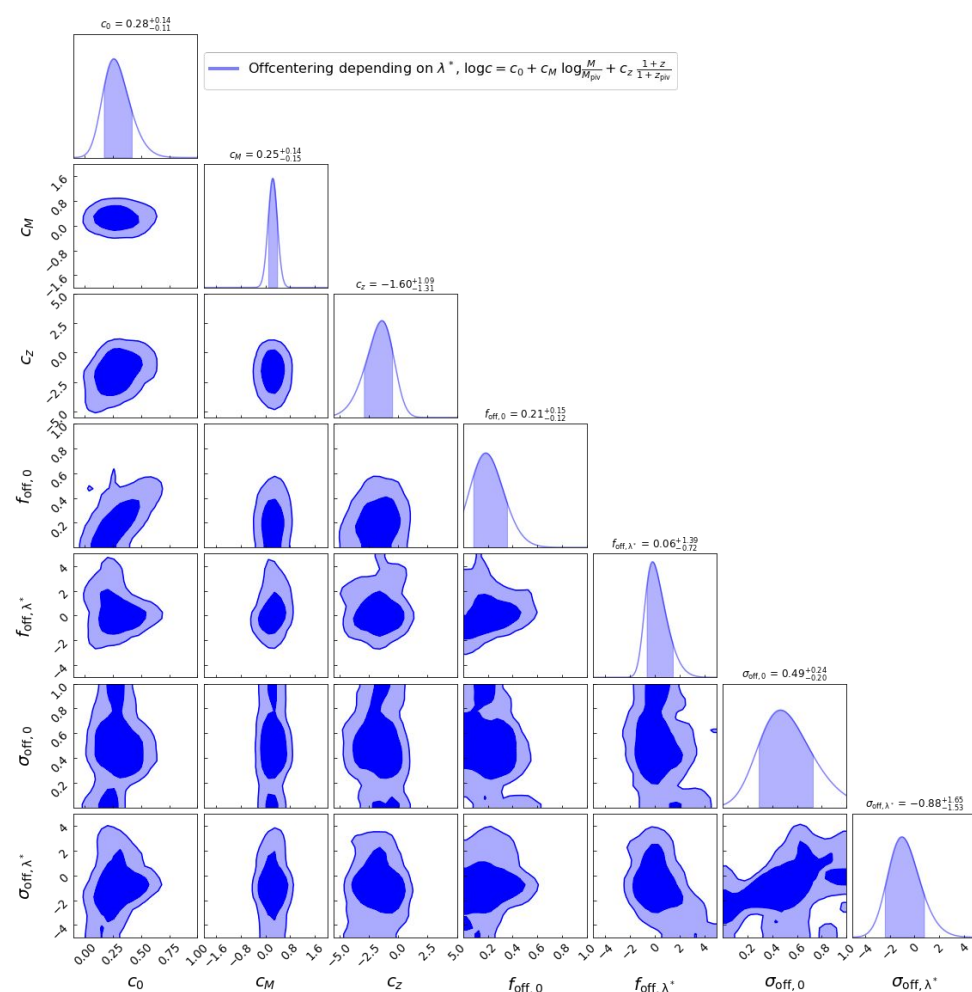
AMICO clusters in KiDS-DR4

Weak lensing mass calibration

(Lesci et al. in prep. 1)

Test: constraining

- mass - richness rel.
- mass - conc. rel.
- offcentering



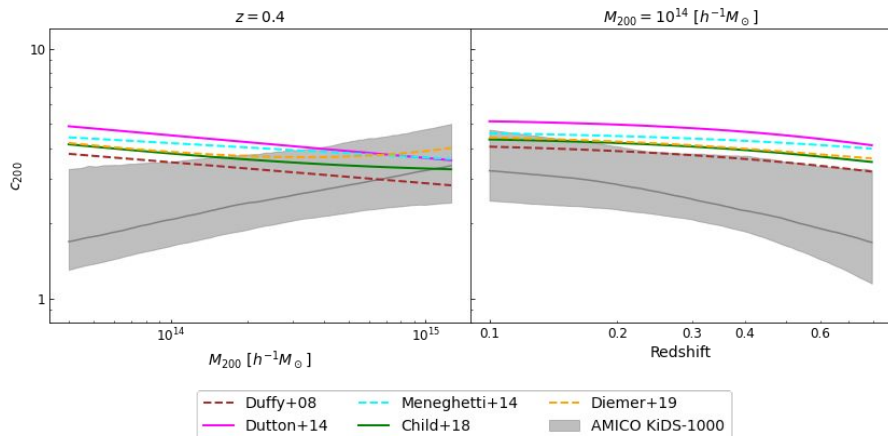
AMICO clusters in KiDS-DR4

Weak lensing mass calibration (Lesci et al. in prep. 1)

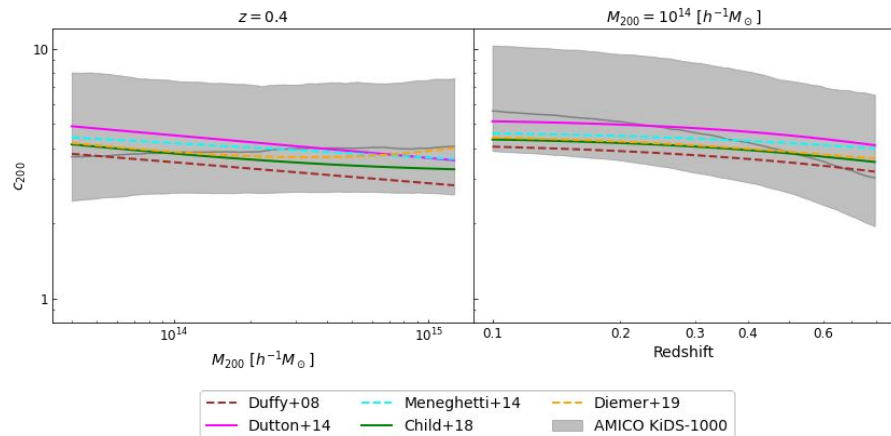
concentration-mass relation:

$$\log c = c_0 + c_M \log \frac{M}{10^{14} M_\odot / h} + c_z \log \frac{1+z}{1+z_{\text{piv}}}$$

BMO, 1-halo + 2-halo



NFW, 1-halo + 2-halo



Colour selections with ground and Euclid bands (Lesci et al. in prep. 2)

$$\begin{aligned}
 x &> c_1 \vee \\
 x &< c_2 \vee \\
 y &> c_3 \vee \\
 y &< c_4 \vee \\
 x &> s_1 y + c_5 \vee \\
 x &> s_2 y + c_6 \vee \\
 x &< s_3 y + c_7 \vee \\
 x &< s_4 y + c_8,
 \end{aligned} \tag{1}$$

where \vee is the "or" logic operator, x and y are two different colours, while the parameters $c_1, \dots, c_8 \in (-\infty, +\infty)$, s_1 and s_3 range in the interval $(0, +\infty)$, while s_2 and s_4 range in the interval $(-\infty, 0)$. We remark that the edges of the aforementioned parameter ranges are excluded. We also stress that Eq. (1) defines an octagonal region where the foreground galaxies can be contained. Thus, for each condition in Eq. (1), we derived the

$$N_{\text{cond}} = 8 \frac{N_{\text{col}}!}{(N_{\text{col}} - 2)! 2!},$$

where N_{col} is the number of colours, expressed as

$$N_{\text{col}} = \frac{N_{\text{band}}!}{(N_{\text{band}} - 2)! 2!},$$

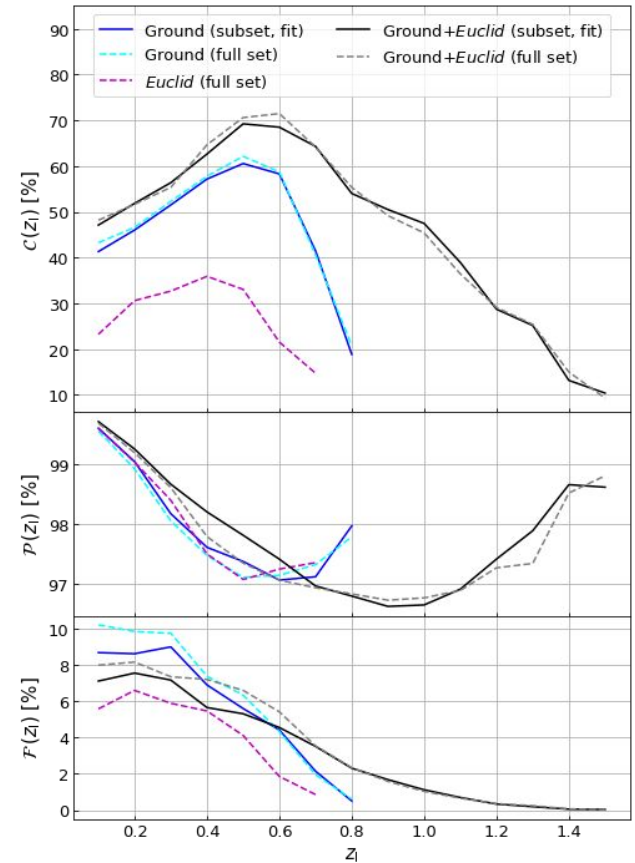
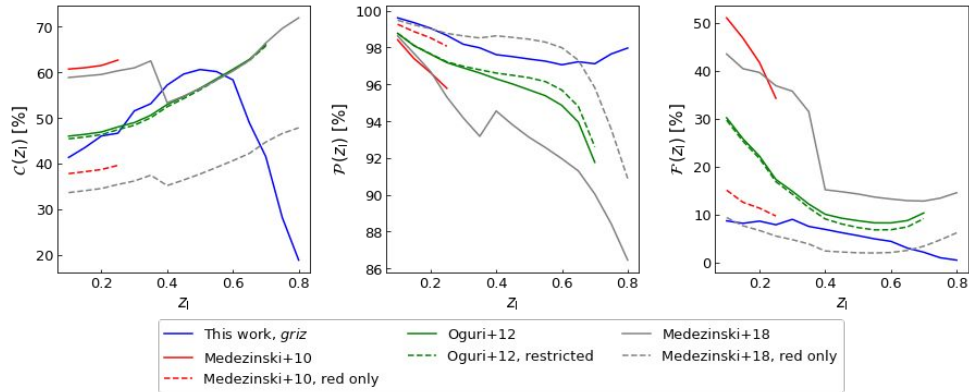
Colour condition	Parameters	z_1 range
$(g-r) < s(r-z) + c$	$s = 22.80 z_1^3 - 24.42 z_1^2 + 6.67 z_1 + 1.13; c = -36.48 z_1^3 + 37.52 z_1^2 - 9.52 z_1 - 0.56$	[0.1, 0.7]
$(g-r) < s(i-z) + c$	$s = 6.72 z_1^2 - 6.84 z_1 + 2.79; c = -6.61 z_1^2 + 6.51 z_1 - 1.70$	[0.1, 0.8]
$(g-r) < s(g-i) + c$	$s = -0.72 z_1^2 + 0.54 z_1 + 0.72; c = 0.01 z_1 - 0.44$	[0.1, 0.6]
$(g-i) > s(i-z) + c$	$s = 0.49; c = 0.50 z_1 + 1.51$	[0.1, 0.3]
$(r-i) < s(r-z) + c$	$s = -1.58 z_1^2 + 0.62 z_1 + 1.63; c = -0.66 z_1^2 + 1.26 z_1 - 1.55$	[0.1, 0.8]
$(g-i) < s(r-i) + c$	$s = 0.19 z_1 + 1.54; c = -7.58 z_1^2 + 6.51 z_1 - 1.43$	[0.3, 0.6]
$(g-i) < s(r-z) + c$	$s = -10.12 z_1^3 + 11.68 z_1^2 - 3.82 z_1 + 1.95; c = -1.21 z_1^2 + 1.38 z_1 - 0.94$	[0.1, 0.8]
$(g-r) > s(i-z) + c$	$s = -3.38 z_1 + 1.02; c = 1.01 z_1 + 0.86$	[0.1, 0.2]
$(g-r) < s(r-i) + c$	$s = 2.59 z_1^2 - 1.69 z_1 + 1.83; c = -4.15 z_1^2 + 3.22 z_1 - 1.17$	[0.1, 0.6]
$(r-i) > s(r-z) + c$	$s = 4.14 z_1^2 - 3.67 z_1 - 0.61; c = 4.70 z_1^2 - 1.93 z_1 + 2.05$	[0.1, 0.6]
$(g-z) < s(r-z) + c$	$s = 1.23 z_1^2 - 0.95 z_1 + 1.77; c = -53.57 z_1^3 + 74.48 z_1^2 - 36.19 z_1^2 + 7.77 z_1 - 0.94$	[0.1, 0.7]
$(i-z) > c$	$c = 1.22 z_1^2 - 0.68 z_1 + 0.70$	[0.1, 0.6]
$(r-i) > s(r-z) + c$	$s = 0.69 z_1^2 - 0.51 z_1 + 0.39; c = 1.44 z_1^2 - 0.66 z_1 + 0.51$	[0.1, 0.5]
$(g-r) < c$	$c = -0.12 z_1 + 0.10$	[0.3, 0.5]

Colour condition	Parameters	z_1 range
$(g-z) < s(i-H) + c$	$s = -0.48 z_1^2 + 0.10 z_1 + 1.56; c = -0.66 z_1^2 + 1.26 z_1 - 1.32$	[0.1, 1.3]
$(g-r) < s(r-z) + c$	$s = 8.05 z_1^3 - 7.59 z_1^2 + 1.44 z_1 + 1.64; c = -22.45 z_1^3 + 20.44 z_1^2 - 3.57 z_1 - 1.49$	[0.1, 0.7]
$(g-Y) < s(z-H) + c$	$s = 1.65; c = -0.28 z_1^2 - 0.11 z_1 - 0.55$	[0.1, 1.5]
$(g-i) < s(r-J) + c$	$s = -0.53 z_1 + 1.29; c = -1.91 z_1^2 + 2.72 z_1 - 1.51$	[0.1, 1.0]
$(r-i) > c$	$c = 2.11 z_1^2 - 1.43 z_1 + 1.03$	[0.1, 0.6]
$(g-i) < s(z-J) + c$	$s = 0.67 z_1^2 - 0.86 z_1 + 1.75; c = -1.33 z_1^2 + 1.56 z_1 - 1.02$	[0.2, 1.3]
$(g-i) < s(i-H) + c$	$s = 0.52 z_1^2 - 1.02 z_1 + 1.57; c = -2.54 z_1^2 + 3.22 z_1 - 1.83$	[0.1, 1.1]
$(g-J) < s(r-H) + c$	$s = 0.34 z_1^2 - 0.48 z_1 + 1.60; c = -14.03 z_1^3 + 14.07 z_1^2 - 2.93 z_1 - 0.97$	[0.1, 0.7]
$(g-r) < s(i-Y) + c$	$s = 1.33 z_1^2 - 1.48 z_1 + 1.81; c = -5.05 z_1^3 + 4.77 z_1^2 - 0.12 z_1 - 1.24$	[0.1, 1.0]
$(g-i) > s(r-Y) + c$	$s = -2.41 z_1 + 0.78; c = 3.03 z_1 + 0.86$	[0.1, 0.2]
$(g-r) < s(Y-H) + c$	$s = 0.86 z_1^2 - 1.57 z_1 + 1.83; c = -3.02 z_1^2 + 2.98 z_1 - 1.22$	[0.1, 0.7]
$(g-i) < s(z-H) + c$	$s = 0.89 z_1^2 - 1.58 z_1 + 1.83; c = -2.26 z_1^2 + 2.58 z_1^2 + 0.14 z_1 - 1.04$	[0.1, 1.3]
$(g-r) < s(i-H) + c$	$s = -0.26 z_1 + 0.95; c = -2.28 z_1^2 + 2.42 z_1 - 1.22$	[0.1, 0.9]
$(g-z) < s(i-J) + c$	$s = -2.02 z_1^2 + 3.65 z_1^2 - 1.83 z_1 + 1.86; c = -0.95 z_1^2 + 1.20 z_1 - 1.12$	[0.1, 1.2]
$(g-z) < s(z-H) + c$	$s = 0.05 z_1 + 1.56; c = -0.64 z_1^2 + 0.27 z_1 - 0.94$	[0.1, 1.4]
$(r-z) > s(i-z) + c$	$s = -3.97 z_1^2 + 0.91 z_1 - 0.41; c = 8.12 z_1^2 - 5.14 z_1 + 2.25$	[0.2, 0.7]
$(g-r) < s(z-J) + c$	$s = 1.49 z_1^2 - 1.54 z_1 + 1.64; c = -2.80 z_1^2 + 2.58 z_1 - 1.11$	[0.1, 1.1]
$(r-i) > s(z-J) + c$	$s = 2.41 z_1^2 - 1.98 z_1 + 0.69; c = 0.66$	[0.2, 0.5]
$(g-Y) < s(i-H) + c$	$s = -0.16 z_1^2 + 0.14 z_1 + 1.66; c = -1.48 z_1^2 + 1.39 z_1 - 1.20$	[0.1, 1.1]
$(g-H) < s(r-H) + c$	$s = -0.34 z_1^2 + 0.17 z_1 + 1.59; c = -0.72 z_1^2 + 1.01 z_1 - 0.96$	[0.1, 0.7]
$(g-i) < s(i-J) + c$	$s = 1.00 z_1^2 - 1.12 z_1 + 1.81; c = -3.30 z_1^2 + 3.62 z_1 - 1.95$	[0.1, 1.1]
$(g-i) < s(r-z) + c$	$s = 0.63 z_1^2 - 0.63 z_1 + 1.80; c = -4.87 z_1^2 + 4.73 z_1 - 1.86$	[0.2, 0.7]
$(g-r) > s(r-i) + c$	$s = -9.65 z_1 + 1.20; c = 8.08 z_1 + 0.05$	[0.2, 0.3]
$(g-i) < s(r-H) + c$	$s = -0.69 z_1^2 + 0.30 z_1 + 0.91; c = -0.65 z_1^2 + 1.30 z_1 - 1.13$	[0.1, 1.0]
$(i-Y) > s(z-Y) + c$	$s = 0.57 z_1^2 - 0.61 z_1 + 0.53; c = 0.60 z_1^2 - 0.42 z_1 + 0.92$	[0.2, 0.8]
$(g-H) < s(i-H) + c$	$s = -0.01 z_1 + 1.69; c = -1.19 z_1^2 + 1.31 z_1 - 0.73$	[0.1, 1.0]
$(r-H) > s(i-J) + c$	$s = 11.03 z_1^2 - 6.52 z_1 + 1.56; c = -12.99 z_1^2 + 7.19 z_1 + 0.70$	[0.1, 0.5]
$(r-z) > s(z-J) + c$	$s = -0.95 z_1^2 + 0.58 z_1 + 0.35; c = 1.62 z_1^2 - 1.22 z_1 + 1.19$	[0.1, 0.6]
$(g-r) < s(z-H) + c$	$s = 4.07 z_1^2 - 4.11 z_1 + 1.83; c = -4.85 z_1^2 + 0.22 z_1^2 + 3.61 z_1 - 1.59$	[0.1, 0.9]
$(g-J) < s(i-H) + c$	$s = -0.57 z_1^2 + 0.72 z_1 + 1.47; c = -2.04 z_1^2 + 2.06 z_1 - 1.17$	[0.3, 0.9]
$(r-i) > s(z-Y) + c$	$s = 1.38 z_1^2 - 1.02 z_1 + 0.47; c = 0.76$	[0.1, 0.5]
$(r-i) < s(z-J) + c$	$s = 1.21 z_1^2 - 2.82 z_1 + 3.32; c = -5.05 z_1^2 + 11.01 z_1 - 7.64$	[1.0, 1.3]
$(g-r) < s(r-Y) + c$	$s = 1.21 z_1^2 - 1.57 z_1 + 1.56; c = -3.61 z_1^2 + 4.04 z_1 - 2.07$	[0.1, 0.7]
$(g-H) > s(i-H) + c$	$s = -0.97 z_1 + 1.55; c = 1.01 z_1 + 1.16$	[0.1, 0.2]
$(g-z) < s(r-z) + c$	$s = 1.21 z_1^2 - 1.04 z_1 + 1.85; c = -2.52 z_1^2 + 2.58 z_1 - 0.99$	[0.3, 0.6]
$(r-i) < s(z-H) + c$	$s = -0.15 z_1 + 1.27; c = -0.22 z_1 - 1.18$	[0.1, 1.1]
$(g-Y) < s(r-J) + c$	$s = -0.69 z_1^2 + 0.46 z_1 + 1.62; c = -1.74 z_1^2 + 1.48 z_1 - 1.30$	[0.1, 0.7]
$(g-i) < s(g-Y) + c$	$s = 0.02 z_1 + 0.75; c = -0.90 z_1^2 + 0.94 z_1 - 0.78$	[0.3, 0.1]

Colour selections with ground and Euclid bands (Lesci et al. in prep. 2)

Colour selections expressed as a function of “lens” redshift.

- robus wrt magnitude limit changes;
- excellent performance on both simulations (Euclid flagship) and real data (COSMOS, VIPERS)
- valid also in case of a missing photometric band.



Summary

- AMICO KiDS-DR3 cluster sample:
 - counts (Lesci et al. 2022a);
 - 3D clustering (Lesci et al. 2022b);
 - 2D clustering and C_1 (Romanello et al. in prep.);
 - weak lensing 2-halo matter profiles (Giocoli+21, Ingoglia+22).
- AMICO KiDS-DR4 cluster sample (Maturi+ in prep., Lesci+ in prep.):
 - huge improvements in the dataset;
 - joint likelihood describing stacked profiles and cluster statistics;
 - cluster physical properties propagated into the cosmological results;
 - blinding.
- Colour selections based on Euclid and ground photometry, expressed as a continuous function of lens redshift.

Thank you for your attention!